Published in final edited form as:
Cell. 2014 July 3; 158(1): 54–68. doi:10.1016/j.cell.2014.06.007.

Glucose Regulates Mitochondrial Motility via Milton Modification by *O*-GlcNAc Transferase

Gulcin Pekkurnaz[1], **Jonathan C. Trinidad**[2], **Xinnan Wang**[3], **Dong Kong**[4], and **Thomas L. Schwarz**[1,*]

[1]The F.M. Kirby Neurobiology Center, Boston Children's Hospital, and Department of Neurobiology, Harvard Medical School, Boston, MA 02115, USA

[2]Department of Chemistry, Biological Mass Spectrometry Facility, Indiana University, Bloomington, IN 47405, USA

[3]Department of Neurosurgery, Stanford University, Stanford, CA 94304, USA

[4]Division of Endocrinology, Department of Medicine, Beth Isreal Deaconess Medical Center, Harvard Medical School, Boston, MA 02215, USA. Present address: Department of Neuroscience, Tufts University School of Medicine, Boston, MA 02116, USA

SUMMARY

Cells allocate substantial resources towards monitoring levels of nutrients that can be used for ATP generation by mitochondria. Among the many specialized cell types, neurons are particularly dependent on mitochondria due to their complex morphology and regional energy needs. Here, we report a molecular mechanism by which nutrient availability in the form of extracellular glucose and the enzyme *O*-GlcNAc Transferase (OGT), whose activity depends on glucose availability, regulates mitochondrial motility in neurons. Activation of OGT diminishes mitochondrial motility. We establish the mitochondrial motor-adaptor protein Milton as a required substrate for OGT to arrest mitochondrial motility by mapping and mutating the key *O*-GlcNAcylated serine residues. We find that the GlcNAcylation state of Milton is altered by extracellular glucose and that OGT alters mitochondrial motility *in vivo*. Our findings suggest that, by dynamically regulating Milton GlcNAcylation, OGT tailors mitochondrial dynamics in neurons based on nutrient availability.

INTRODUCTION

Mitochondria form a dynamic, interconnected network and play a vital role in cellular energetics by generating ATP, buffering calcium, and participating in metabolic pathways. Positioning mitochondria in areas of high-energy consumption followed by the induction of oxidative phosphorylation can allow cells to respond to increased energy demands.

*Correspondence: Thomas.Schwarz@childrens.harvard.edu.

Therefore, the molecular mechanisms that relay signals to mitochondria about changes in local nutrient status and metabolic demand are critical for cell function (Liesa and Shirihai, 2013; Nunnari and Suomalainen, 2012).

Glucose is the predominant carbon source for ATP production by mitochondria. Neuronal metabolism in particular relies heavily on a continuous supply of glucose (Peppiatt and Attwell, 2004). Moreover, due to their elaborate morphology and regional differences in energy use and nutrient access, glucose uptake and handling is spatially heterogeneous in neurons (Ferreira et al., 2011; Hall et al., 2012; Weisova et al., 2009). Mitochondrial dynamics may therefore need to respond to changes in the glucose supply to ensure rapid ATP production, especially during intense synaptic activity and action potential firing.

The distribution of neuronal mitochondria is determined by the elaborate regulation of their motility (Chang et al., 2006). They can move in either direction, pause, change direction, or remain stationary. This behavior is primarily mediated by the interplay of (+)-end directed kinesin, (−)-end directed dynein motors, and anchoring proteins (Schwarz, 2013).

The mitochondrial motor/adaptor complex plays a central role in regulating this process (Wang and Schwarz, 2009b). The mitochondrial receptor for this complex, the GTPase Miro (also called RhoT1/2), interacts with the adaptor protein Milton (also called TRAK1/2 and OIP106/98), which couples KHC and dynein/dynactin to mitochondria (Glater et al., 2006; Macaskill et al., 2009; van Spronsen et al., 2013). Milton also binds an enzyme called *O*-GlcNAc transferase (OGT) (Iyer et al., 2003; Iyer and Hart, 2003). OGT catalyzes the addition of a single sugar moiety onto serine and threonine residues of nuclear and cytoplasmic proteins, including Milton, in a process called *O*-GlcNAcylation. OGT has been considered a metabolic sensor for glucose (Hart et al., 2011) because *O*-GlcNAcylation levels are influenced by glucose flux via the Hexosamine Biosynthetic Pathway (HBP), which produces the donor substrate, UDP-GlcNAc.

While the OGT/Milton interaction is conserved from *Drosophila* (Glater et al., 2006) to mammals (Brickley et al., 2010; Iyer and Hart, 2003), its functional significance is unknown. We hypothesized that mitochondrial motility would be sensitive to glucose levels and that OGT-dependent Milton *O*-GlcNAcylation links glucose metabolism to the regulation of mitochondrial motility.

RESULTS

Increased Extracellular Glucose Decreases Mitochondrial Motility in Hippocampal Axons

To examine the effects of elevated extracellular glucose on axonal mitochondrial motility, we performed live cell imaging in rat hippocampal neurons expressing Mito-DsRed, a mitochondrial marker, and Synaptophysin-CFP (Syp-CFP), a marker of synaptic vesicle precursors. Normal neurobasal (NB) medium contains a high level of glucose (25mM), which likely saturates glucose transporters. Therefore, we switched established cultures to a pre-conditioning 5mM glucose medium for 70h before challenging them with elevated (30mM) glucose (Figure 1A). Live imaging of a fluorescent glucose sensor (Hou et al., 2011) confirmed that this extracellular shift altered intracellular glucose concentration

(Figure 1B and 1C). The transporter that likely mediates this increase, GLUT3, was present at neuronal cell bodies and densely spaced patches along processes (Figure S1)(Choeiri et al., 2002; Ferreira et al., 2011); mitochondria throughout the cell are therefore likely to experience the shift in intracellular glucose.

To compare their dynamics in neurons maintained in 5mM or shifted to 30mM glucose, we determined the percent time each mitochondrion and Syp-vesicle spent in motion, their average velocity, and total distance traveled, as well as mitochondrial length and density (Table S1). Increasing extracellular glucose reduced both anterograde and retrograde movement of mitochondria (Figure 1D–1F). Mitochondrial density also decreased in axons, potentially due to decreased movement of mitochondria into the axon from the cell body (Table S1A). The reduction was specific to mitochondria; movement of Syp-vesicles in the same axons increased significantly in both directions (Figure 1G; Table S1A) even as mitochondrial movement decreased. The enhanced movement of Syp-vesicles entailed increases in velocity and total distance traveled.

Increased *O*-GlcNAc Transferase Activity Arrests Mitochondria

We hypothesized that OGT was responsible for the effect of elevated glucose on mitochondrial movement. We therefore examined the effect of OGT by transfecting neurons with the full-length nucleocytoplasmic isoforms of OGT together with Mito-DsRed and Syp-CFP. OGT overexpression reduced axonal mitochondrial motility and density (Figure 2, Table S1B). In contrast, OGT did not decrease the movement of Syp-vesicles. Expression of OGT^{H498N}, a mutant lacking catalytic activity, (Lazarus et al., 2011) (Figure S2A) did not significantly change mitochondrial motility (Figure 2C). To increase *O*-GlcNAcylation without overexpressing OGT, we instead treated neurons with *O*-(2-acetamido-2-deoxy-D-glucopyranosylidene)amino-*N*-phenylcarbamate (PUGNAC), an inhibitor of the de-GlcNAcylating enzyme OGA. PUGNAC also reduced mitochondrial motility (Figure 2C). Thus either the expression of catalytically active OGT or the inhibition of endogenous OGA mimicked the effect of elevated glucose on mitochondrial motility.

We also probed the influence of OGT by pharmacologically manipulating the availability of its substrate UDP-GlcNAc. UDP-GlcNAc synthesis can be blocked with 6-diazo-5-oxo-L-norleucine (DON), an inhibitor of Glutamine Fructose-6-phosphate Amidotransferase (GFAT). We therefore cultured hippocampal neurons expressing OGT in 5mM glucose for 72hrs either in the presence or absence of 10μM DON. DON alone did not alter mitochondrial motility but it prevented the inhibition of movement caused by OGT overexpression (Figure S2B–2F). These observations were consistent with a model in which increased glucose availability stimulated OGT activity (Butkinaree et al., 2010; Love and Hanover, 2005) and thereby inhibited the movement of mitochondria.

To assess whether reducing endogenous OGT alters mitochondrial motility, we depleted OGT from neurons by co-expressing GFP with a short hairpin RNA (shRNA) against OGT (Caldwell et al., 2010). The efficacy of the shRNA was established in hippocampal neurons after 4 days of expression (Figure S2G) and in HEK293T cells (Figure S2H). OGT depletion enhanced mitochondrial motility in both directions (Figure 2E–2G, and Table S1B). This enhancement was suppressed by expression of shRNA-resistant OGT (Figure S2I–2J) and

was specific to mitochondria because the retrograde trafficking of late endosomal vesicles (visualized by RFP-Rab7) was inhibited by OGT depletion (Figure S2K).

Regulation of Mitochondrial Motility in the Physiological Range of Glucose Concentrations

Although neurons are normally cultured in 25mM glucose, extracellular glucose ranges from 2–6mM in mammalian brain (Silver and Erecinska, 1994). To examine mitochondrial motility at concentrations resembling those *in vivo*, we cultured hippocampal neurons in 5mM glucose containing NB medium, and then lowered the glucose to 1mM for 48hrs before challenging them with 5mM glucose for 2hrs. 1mM lactate and pyruvate were present throughout as alternative energy supplies that are not metabolized to UDP-GlcNAc. Shifting to higher extracellular glucose again reduced mitochondrial movement (Figure 2I, 2J and 2M). Consistent with mediation by the HBP, the reduction was blocked by DON (Figure 2H–2M). Glucosamine, which enters the HBP downstream of GFAT also reduced mitochondrial movement, and, as predicted, this reduction was not blocked by DON (Figure 2M).

Milton Recruits OGT to Mitochondria and Undergoes Regulated *O*-GlcNAcylation

To determine whether the interaction with Milton caused OGT to be recruited to the mitochondrial surface we transfected both COS7 cells and neurons with Mito-DsRed and eGFP-tagged OGT in the presence and absence of myc-hMilton1. Expression of the tagged OGT allowed us to distinguish mitochondrial binding of the nucleocytoplasmic isoform in the transgene from an intramitochondrial variant that also occurs in cells (Love and Hanover, 2005). In the absence of Milton expression, eGFP-OGT was largely diffuse in the COS7 cytosol and nucleus, although some was present on mitochondria. With Milton overexpression (Figure S3A) eGFP-OGT was highly mitochondrial. Similarly, in neuronal processes eGFP-OGT became highly enriched on mitochondria when Milton was co-expressed (Figure 3A–D). Miro or KHC co-expression did not enrich eGFP-OGT on mitochondria (data not shown).

To test the possibility that OGT arrests mitochondrial motility through dissociation of the Milton/KHC/Miro complex we immunoprecipitated hMilton1 from HEK293T cells with or without overexpression of OGT. Endogenous OGT coprecipitated with hMilton1 but overexpression of OGT greatly enhanced this association (Figure 3E). However, as OGT-hMilton1 association increased, levels of coprecipitated kinesin and Miro remained constant. Moreover, immunoprecipitation of an epitope-tagged kinesin pulled down both endogenous and overexpressed OGT together with hMilton1 (Figure S3B). Thus association of OGT with Milton did not disrupt the mitochondrial motor/adaptor complex (Figure 3E and S3B) and OGT bound to complexes that also contain KHC.

We examined O-GlcNAcylation of myc-tagged hMilton1 to determine whether the extent of its modification was altered when OGT was overexpressed or OGA inhibited. Anti-GlcNAc antibodies detected a band that co-migrated with hMilton1 in anti-myc immunoprecipates from HEK293T cells expressing myc-tagged hMilton1 (Figure 3F). Intensity of this band was increased by inhibition of OGA by PUGNAC, overexpression of OGT, or both combined (Figure 3F and 3G) but overexpression of OGT^{H498N} did not (Figure 3H and 3I).

PUGNAC also increased the GlcNAcylation state of endogenous hMilton1 (Figure S3C). Thus, GlcNAcylation sites on Milton are not saturated in control conditions and the level of their modification is likely to be determined by the balance of OGT and OGA activity.

A Stable OGT-Milton Interaction Is Not Necessary for *O*-GlcNAcylation of Milton

Milton, unlike most other highly *O*-GlcNAcylated proteins, forms a stable immunoprecitatable complex with OGT both *in vitro* and *in vivo* (Brickley et al., 2010; Iyer et al., 2003; Iyer and Hart, 2003). To determine if we could selectively prevent Milton *O*-GlcNAcylation by interfering with this binding, we mapped the region required for its stable association with OGT. We expressed truncated forms of both *Drosophila* MiltonA and hMilton1 in HEK293T cells and assayed their ability to co-precipitate with OGT (Figure 4A, S4A–4C). OGT-binding appeared to depend on residues between 450–750 of *Drosophila* MiltonA (Figure 4A) and 634–953 of hMilton1 (Figure S4A and B). Although these are among the less conserved regions of Milton, we identified a highly conserved 15 amino acid region (658–672 in hMilton1; Figure 4B). Deletion of these residues prevented the coprecipitation of OGT with Milton (Figure 4C). hMilton1 lacking this OGT-Binding Domain (hMilton1ΔOBD) retained the ability to coprecipitate with KHC and Miro and localize to mitochondria (Figure S4C–S4E). However, although hMilton1ΔOBD no longer bound OGT with sufficient affinity to coprecipitate, its *O*-GlcNAcylation by OGT was not diminished but rather increased indicating that the high-affinity interaction interferes with its ability to modify Milton (Figure 4D and 4E). Thus, formation of a stable OGT-Milton complex is not required for Milton to serve as a substrate for OGT. The tetratricopeptide repeat (TPR) domains of OGT, however, are thought to scaffold the interactions of OGT with multiple substrates (Iyer and Hart, 2003; Lazarus et al., 2011). Deletion of the first 6 TPR domains (Δ6 TPR) decreased Milton *O*-GlcNAcylation, as anticipated (Figure 4F–4H) and this truncated OGT did not arrest neuronal mitochondria (Figure 4I–4K and Table S1C). Thus the GlcNAcylation of Milton does not require the exceptionally stable interaction of OGT with the OBD domain on Milton, but, as with other OGT substrates, requires the substrate-recognizing TPR domains of OGT.

OGT-Dependent Mitochondrial Arrest Requires Milton *O*-GlcNAcylation

We previously characterized four sites of *O*-GlcNAcylation on Milton isolated from mouse synaptosomes (Trinidad et al., 2012). To identify O-GlcNAcylation sites present in hMilton1, this protein was immunoprecipitated from HEK293T cells and resolved on an SDS-PAGE gel. Peptides isolated from a tryptic digestion were analyzed by MS/MS using electron transfer dissociation, which preserves labile glycosidic linkages. We identified eight peptides on hMilton1 that were modified with O-GlcNAc. In three of these, the modified site could be localized to a single residue (Figure S5).

To determine the potential role of these sites in mitochondrial arrest, we expressed in HEK293T cells hMilton1 constructs wherein putative *O*-GlcNAcylation sites were mutated to alanine (Figure S5 and Table S1D) and measured their relative *O*-GlcNAc levels. We focused on four *O*-GlcNAcylated serines conserved between mouse and human Milton1 (Figure 5A). Mutation of any of the four sites reduced the amount of GlcNAc immunoreactivity present on Milton (Figure 5B). The requirement for Milton *O*-

GlcNAcylation in mediating the OGT-dependent mitochondrial arrest was demonstrated with a quadruple mutant that had all four of these conserved serines changed to alanine (hMilton1^{Qmut}).

We compared the consequences of its expression to that of hMilton1 WT when OGT was co-expressed. Therefore, we used hMilton1 DNA at a low concentration (0.2μg/well of a 24-well plate) to minimize the increase in motility caused by high levels of Milton (Glater et al., 2006). By immunostaining, 96±2.27% of neurons that were Mito-DsRed positive were also myc-hMilton1 and OGT positive (Figure S5I). The quadruple mutation, expressed on its own, increased mitochondrial length by 20% but had little effect on the parameters of mitochondrial movement when compared to wildtype Milton expression (Table S1E) and therefore allowed a straightforward comparison of the effect of OGT expression on mitochondria bearing either form of Milton. Three concentrations of OGT DNA were used for transfections so as to construct a dose/response relationship. As expected, mitochondrial motility decreased in both control and hMilton1 WT-expressing neurons as we increased the amount of transfected OGT DNA (Figure 5D, 5E and 5H, Table S1E). However, when hMilton1^{Qmut} was expressed, OGT expression had no effect on their motility, even when the highest concentration of OGT DNA was transfected (Figure 5F–5H and Table S1E). hMilton1^{Qmut} prevented the arrest whether or not the endogenous murine Milton was knocked down by shRNA (Figure S5J and 5K). We also analyzed mitochondrial motility in neurons expressing hMilton1 S447A, S829/30A or S938A together with OGT overexpression or PUGNAC treatment (Figure S5L). The individual mutations were also effective in rendering motility resistant to OGT. Understanding the significance of individual sites will require further elucidation of this mechanism.

Glucose-Dependent Changes in Mitochondrial Motility Require Milton *O*-GlcNAcylation

Identification of the required *O*-GlcNAcylation sites on hMilton1 allowed us to use the protocol in Figure 1A to determine whether this modification mediated the effect of increased extracellular glucose. High glucose decreased movement in hippocampal neurons expressing WT hMilton1 (Figure 6A, 6B and 6E, Table S1F). In contrast, motility increased in neurons expressing hMilton1^{Qmut} (Figure 6C–E, Table S1F), particularly in the anterograde direction. Thus the suppression of mitochondrial movement is mediated by the GlcNAcylation of Milton. In its absence, mitochondria behave akin to the Syp-vesicles of Figure 1, whose motility was enhanced when more glucose was available. To determine the *O*-GlcNAcylation state of Milton under different extracellular glucose conditions, we expressed myc-tagged WT or Qmut hMilton1 constructs in HEK293T cells. High glucose only increased the *O*-GlcNAcylation level of WT hMilton1 (Figure 6F and 6G).

Loss of OGT Decreases the Stationary Mitochondrial Pool *in vivo*

Because the interaction of OGT with Milton is conserved (Figure 4A)(Glater et al., 2006), we took advantage of available *Drosophila* lines to ask whether OGT was regulating mitochondrial movement *in vivo*. A *piggy*Bac insertion into the *ogt* coding sequence (*ogt*$^{-/-}$) (Schuldiner et al., 2008; ID:LL01151) abolished detectable OGT protein (Figure S6A). Individual axons in segmental nerves (Schuldiner et al., 2008; Wang and Schwarz, 2009a) of *ogt*$^{-/-}$ larvae had fewer stationary mitochondria (Figure 7A–7C) and fewer

mitochondria per micron of axon than control larvae (Figure S6B). These results *in vivo* in Drosophila parallel the effects of OGT knockdown in cultured hippocampal neurons and indicate a conserved role of O-GlcNAc cycling in regulating mitochondrial motility.

Milton *O*-GlcNAcylation Levels in Mouse Brain are Altered by Feeding

In tissue culture, changes in extracellular glucose altered the extent of Milton GlcNAcylation (Figure 6F and 6G). To determine if it also varied *in vivo* we took advantage of the fact that the concentration of extracellular glucose in the brain changes in parallel with blood glucose during fasting and feeding cycles (Silver and Erecinska, 1994). Mice were either; 1) fed *ad libitum*, 2) fasted for 24h or 3) fasted for 24h and then returned to food for 24h (Figure 7D) after which their blood glucose was monitored and cerebral cortices removed to measure Milton *O*-GlcNAcylation (Figure 7E and 7F). Although the drop in blood glucose that accompanied fasting did not produce a parallel decrease in Milton GlcNAcylation, refeeding following the fasting significantly increased it.

Axonal Mitochondria Accumulate in Areas of Higher Glucose

One possible consequence of the OGT pathway is that moving mitochondria would tend to stop where cytosolic glucose is elevated. To determine whether spatial inhomogeneities of glucose could alter mitochondrial distribution in an axon, we used microfluidic chambers to create a boundary between a zone with 5mM glucose and one with glucose-free medium, (Figure 7G and S6C). Because the glucose transporter will effectively clamp the local cytoplasmic concentration at equilibrium with the external glucose, a local difference in cytoplasmic glucose should also arise. Hippocampal neurons were cultured in chambers in 5mM glucose and allowed to grow their axons through 0.45mm grooves into an axonal chamber (Figure 7G). Trypan blue was used to confirm that fluidic isolation of the axonal compartment was preserved during medium exchanges (Figure S6C). To create the glucose differential, the somal compartment was switched to glucose-free medium while the axonal compartment remained in 5mM glucose. A stretch of axon on the 5mM glucose side of the glucose discontinuity was imaged before and after the solution change (Figure 7G). Lowering glucose in the somal compartment caused an accumulation of mitochondria in this adjacent area of higher glucose (Figure 7I and 7J). This accumulation is consistent with a model in which the mobile mitochondria from the glucose-free compartment arrest when they encounter the region with higher glucose.

DISCUSSION

Mitochondria movement controls their distribution in cells, their likelihood of fusing, and their rate of turnover in the cell periphery. The control of mitochondrial movement can therefore influence energy, signaling, metabolism, and Ca^{2+} buffering in different regions of a cell (Saxton and Hollenbeck, 2012). We have now established 1) that extracellular glucose regulates mitochondrial dynamics, 2) that the enzyme OGT, a putative metabolic sensor, mediates this effect, 3) that a post-translational modification of Milton is an absolutely required target of this enzyme, and 4) that the pathway is likely to be physiologically relevant in vivo for regulating mitochondrial dynamics and distribution.

The GlcNAcylation level of Milton correlated well with mitochondrial motility, whether the level was manipulated by overexpression or knockdown of OGT, or by pharmacological inhibition of OGA or UDP-GlcNAc synthesis (Figures 2). OGT has many substrates, including several such as tubulin, kinesin and dynein with potential impact on mitochondrial dynamics (Ji et al., 2010; Ruan et al., 2012; Trinidad et al., 2012). However, by mapping and mutating four key sites of GlcNAc addition in hMilton1 (hMilton1^{Qmut}), we demonstrated that Milton is the key and essential substrate through which OGT inhibits mitochondrial motility. These mutations had little effect on the baseline properties of mitochondrial movement but selectively prevented the arrest by OGT (Figure 5). With hMilton1^{Qmut} expression we also found that GlcNAcylation of Milton mediated the decrease in mitochondrial movement caused by elevated extracellular glucose (Figure 6). Moreover, although in this study we took advantage of the polarized arrays of microtubules in axons, the components of this pathway are present in all metazoan cells and glucose, via OGT, may therefore be a widespread regulator of mitochondrial movement.

Protein GlcNAcylation is a posttranslational modification that occurs on over 1,000 proteins and has received much recent attention (Ruan et al., 2013). OGT has low-affinity interactions with many of its substrates but forms a stable complex with few. Milton was one of the first identified high-affinity OGT partners (Iyer et al., 2003; Iyer and Hart, 2003) and we have identified a 15 amino acid region in hMilton1 (aa 658–672) that is required for stable OGT-Milton complexes (Figure 5 and S4). However, deletion of this region does not reduce hMilton1 O-GlcNAcylation (Figure 5D) on the critical sites. A similar dissociation of OGT binding and *O*-GlcNAcylation has been described for HCF-1 (Capotosti et al., 2011). OGT-Milton complexes may facilitate OGT transport throughout cells or target OGT to the mitochondrial surface (Figure S3) for additional metabolic regulation.

O-GlcNAcylation, like phosphorylation, modifies serine and threonine side chains and crosstalk and competition between phosphorylation and *O*-GlcNAcylation may be important for some substrates (Hart et al., 2011). 28 hMilton1 phosphorylation sites have been previously identified (Hornbeck et al., 2012) and we have mapped additional sites, however no phosphorylation has been found at the critical *O*-GlcNacylation sites that regulate mitochondrial motility.

Some GlcNAcylation sites turn over very slowly and may serve a primarily structural role while others are actively cycled and likely regulate protein function (Khidekel et al., 2007). Only for the latter class will PUGNAC inhibition of OGA cause the level of *O*-GlcNAcylation to rise (Khidekel et al., 2007; Matthews et al., 2007; Yi et al., 2012). Milton modification meets this criterion (Figure 3F and G) and OGA inhibition decreased mitochondrial motility (Figure 2C). Thus the GlcNAc sites on Milton are undergoing dynamic regulation and normally exist in a substoichiometric level of modification that allows the motor/adaptor complex to respond to changes in glucose availability.

The inhibitory effect of increased extracellular glucose on mitochondrial movement was not shared by Syp-vesicles in the same axons although both organelles use dynein for retrograde movement. Indeed, the movement of Syp-vesicles was increased when glucose was raised (Figure 1). Mechanistically, this distinction is explained by two factors. 1) The locus of the

inhibitory regulation is not in the motors themselves but in Milton, which is specific to mitochondria. 2) Changing extracellular glucose from 5.5 to 30mM has been calculated to increase ATP three-fold in hippocampal neurons (Huang et al., 2007) and raising ATP levels enhances the activity of kinesin and dynein, which require ATP hydrolysis for force generation (Fort et al., 2011; Visscher et al., 1999). Therefore, in the absence of the overriding influence of Milton GlcNAcylation, cargo transport will increase with increased glucose availability, a phenomenon we also observed for mitochondria when the action of OGT was prevented by expression of hMilton1^{Qmut} (Figure 6). Local microdomains of ATP can affect the velocity and extent of vesicle motility and organelles can increase the efficiency of their transport by carrying their own ATP-generating machinery and mitochondrial motors require ATP produced by mitochondria (Zala et al., 2013).

The OGT pathway can now be added to a growing list of signaling cascades that regulate the motile pool of mitochondria, including changes in cytosolic Ca^{2+} (Macaskill et al., 2009; Wang and Schwarz, 2009b), growth factors and their downstream kinases (Chada and Hollenbeck, 2003), hypoxia (Li et al., 2009), Armcx (Lopez-Domenech et al., 2012) and the PINK1/Parkin pathway (Wang et al., 2011). It is noteworthy, however, that although each of these pathways can increase the number of stationary mitochondria, they do not account for the majority of stationary mitochondria in an axon. In Drosophila lacking OGT, 60% of the mitochondria remained stationary (Figure 7A–C). Similarly, ~60% of axonal mitochondria remained stationary upon knockdown of OGT or block of UDP-GlcNAc synthesis (Figure 2) and a similar fraction is stationary upon expression of Ca^{2+}-resistant Miro or mutation of PINK1 or Parkin (Wang and Schwarz, 2009b; Wang et al., 2011). This persistently stationary mitochondrial pool is dependent on anchoring proteins including Syntaphilin (Kang et al., 2008) and Myosin VI (Pathak et al., 2010). This distinction between anchored mitochondria unchanged by short-term signals and a mobile pool that can be arrested when necessary may help the cell balance an adequate baseline of mitochondria throughout the cell while fine-tuning their distribution via the mobile pool as nutrient supply and energetic demand fluctuate.

In this study, we determined that the OGT/*O*-GlcNAcylation pathway enables neuronal mitochondrial motility to respond to changes in glucose availability. Although most measurements were conducted in cultured cells where glucose availability can readily be altered, our data indicate that the pathway also functions *in vivo*. In Drosophila, removal of OGT increased the fraction of mobile mitochondria demonstrating that there is a tonic inhibition by the OGT pathway (Figure 7A–C). In addition, we demonstrated that the extent of GlcNAcylation of Milton in mouse brain *in vivo* could vary: the increase in glucose availability upon feeding previously fasted mice increased the level of Milton *O*-GlcNAcylation (Figure 7D–F). In principle, the pathway *in vivo* could respond to either spatial differences or temporal changes in glucose concentration and has the potential to enrich mitochondria in subcellular locations of high glucose for efficient ATP production. Indeed, when we created a differential in glucose concentration in microfluidic chambers, mitochondrial density increased where glucose was high. Little is known about cytoplasmic glucose concentrations in neurons, but the inhomogeneous distribution of glucose transporters (Gerhart et al., 1992) and OGT and OGA (Akimoto et al., 2003; Cole and Hart,

2001; Tallent et al., 2009) *in vivo* suggests that both the glucose supply and key enzymes may be heterogeneously distributed. In addition, some parts of neurons likely have better access to extracellular glucose, such as nodes of Ranvier or areas close to blood vessels. Altered distribution of mitochondria is only one likely consequence; because mitochondrial fusion is highly dependent on their motility, increased Milton GlcNAcylation is likely to decrease fusion and the exchange of components and have consequences for metabolism (Liesa and Shirihai, 2013; Liu and Hajnoczky, 2011). Temporal changes in glucose availability are also relevant to neuronal metabolism. In both the central and peripheral nervous system, fasting and feeding alters levels of extracellular glucose (Choeiri et al., 2002; Dash et al., 2013; Silver and Erecinska, 1994). Furthermore, during synaptic activity and action potential firing, surface glucose transporter levels and hence glucose uptake is increased, as is ATP consumption (Ferreira et al., 2011; Weisova et al., 2009). Thus, during intense synaptic activity, the local activation of OGT and *O*-GlcNAcylation of Milton would cause existing mitochondria to be retained at pre- and postsynaptic sites and would capture any nearby transiting mitochondria. The resulting enrichment for mitochondria would ensure ATP production and Ca^{2+} buffering to preserve synaptic efficacy. On the other hand, poorly regulated blood glucose give rise to diabetic neuropathy and it is tempting to speculate that misregulation of mitochondrial motility in peripheral axons, via the pathway described here, could cause insufficient turnover of peripheral mitochondria and thereby contribute to axonal degeneration.

EXPERIMENTAL PROCEDURES

Plasmid constructs

Standard PCR-based cloning strategies were used (see Extended Experimental Procedures).

Cell culture and Transfection

HEK293T and COS7 cells were cultured in DMEM supplemented with L-glutamine, penicillin/streptomycin (Life Technologies) and 10% FBS (Atlanta Premium). Plasmid DNA transfections were performed with the calcium phosphate method. When used, PUGNAC (Tocris Bioscience) was applied at 100μM for 12–20hrs before cell lysis.

Hippocampal neurons were isolated from E18 rat (Charles River) embryos as previously described (Nie and Sahin, 2011) and plated at $5–7\times10^4/cm^2$ density on coverslips (Bellco Glass, Inc.) coated with 20 μg/ml poly-L-ornithine (Sigma) and 3.5 μ/ml laminin (Life Technologies) and maintained in Neurobasal (NB) medium supplemented with B27 (Life Technologies) and L-glutamine, penicillin/streptomycin, unless modified as specified. 7–10DIV hippocampal neurons were transfected using Lipofectamine2000 (Life Technologies) and imaged 2–3 days later. The coexpression of multiple constructs transfected into neurons was validated by retrospective immunostaining following live cell imaging. For particular treatments of neuronal cultures see Extended Experimental Procedures.

Live cell imaging and motility analysis

For live cell imaging of axonal mitochondria and Syp-vesicles, coverslips were transferred to HibernateE (BrainBits) medium to maintain cell viability in CO_2 free conditions.

Kymographs were generated from 3–5min long time-lapse movies and analyzed with Kymolyzer, a custom-written ImageJ macro (see Extended Experimental Procedures for details) for percent time in motion, velocity, total distance traveled, mitochondrial density, and length.

Immunocytochemistry and Protein Analyses

Hippocampal neurons and COS7 cells were fixed and immunostained as previously (Glater et al., 2006; Stowers et al., 2002) with the indicated antibodies (see Extended Experimental Procedures). Images were processed with ImageJ (Schneider et al., 2012) using only linear adjustments of contrast and color. HEK293T cells lysis and immunoprecipitations were performed as previously with minor modifications (Glater et al., 2006). For immunodetection and hMilton1 GlcNAcylation measurements from immunoprecipitates, see Extended Experimental Procedures.

Drosophila stocks and mitochondrial motility analysis

The following *Drosophila* stocks were used; *CCAP-GAL4* (Park et al., 2003), *UAS-mito-GFP* (Pilling et al., 2006), $ogt^{-/-}$ (Schuldiner et al., 2008). Dissected third-instar larvae were imaged in a chamber on a glass slide. Kymographs were generated and analyzed as described previously (Wang and Schwarz, 2009a).

Statistical analysis

Throughout the paper data are expressed as the mean ± SEM. Statistical analysis was performed with GraphPad Prism v6.0 for MacOSX. The Mann-Whitney *U* test was used to determine the significance of differences between two conditions. Multiple conditions were compared by Kruskal-Wallis non-parametric ANOVA test, which was followed by Dunn's multiple comparisons test or by One-way ANOVA with post hoc Tukey's test as appropriate to determine significance of differences across every condition to control condition. $p < 0.05$ was considered significant.

Supplementary Material

Refer to Web version on PubMed Central for supplementary material.

Acknowledgments

We gratefully acknowledge the gift of plasmid constructs from: Drs. P. Aspenström for myc-hMiro1/2; G. Hajnóczky for Mito-DsRed; G.W. Hart for OGT and Xpress-hMilton1; X. Yang for eGFP-OGT; H.T. Cline for Syp-CFP; M. Sahin for scrambled shRNA; M.J. Reginato for OGT shRNA; K.J. Verhey for KHC-mCit; M. Greenberg for pEGFP-N1. We thank S. Vasquez, K. Pereira, K. Apaydin and Dr. M. Sahin's laboratory for assistance with primary hippocampal neuron cultures; X. Ho, E. Ling and Y. Guo for technical assistance; L. Ding from Harvard NeuroDiscovery Center, Enhanced Neuroimaging Core for assistance with development of Kymolyzer; the IDDRC Molecular Genetics and Imaging Cores (grant number P30HD18655). We also thank Drs. M. Banghart, R. Cartoni, M.A. Cronin, B. Lowell, G. Yellen, and M. Tantama,, and A. Nasser and M. Hamilton for support and valuable input. D.K. was supported by K01DK094943 and P30DK46200. This work was supported by 5R01GM069808-08 and the Ellison Medical Foundation.

References

Akimoto Y, Comer FI, Cole RN, Kudo A, Kawakami H, Hirano H, Hart GW. Localization of the O-GlcNAc transferase and O-GlcNAc-modified proteins in rat cerebellar cortex. Brain Res. 2003; 966:194–205. [PubMed: 12618343]

Brickley K, Pozo K, Stephenson FA. N-acetylglucosamine transferase is an integral component of a kinesin-directed mitochondrial trafficking complex. Biochim Biophys Acta. 2010; 1813:269–281. [PubMed: 21034780]

Butkinaree C, Park K, Hart GW. O-linked beta-N-acetylglucosamine (O-GlcNAc): Extensive crosstalk with phosphorylation to regulate signaling and transcription in response to nutrients and stress. Biochim Biophys Acta. 2010; 1800:96–106. [PubMed: 19647786]

Caldwell SA, Jackson SR, Shahriari KS, Lynch TP, Sethi G, Walker S, Vosseller K, Reginato MJ. Nutrient sensor O-GlcNAc transferase regulates breast cancer tumorigenesis through targeting of the oncogenic transcription factor FoxM1. Oncogene. 2010; 29:2831–2842. [PubMed: 20190804]

Capotosti F, Guernier S, Lammers F, Waridel P, Cai Y, Jin J, Conaway JW, Conaway RC, Herr W. O-GlcNAc transferase catalyzes site-specific proteolysis of HCF-1. Cell. 2011; 144:376–388. [PubMed: 21295698]

Chada SR, Hollenbeck PJ. Mitochondrial movement and positioning in axons: the role of growth factor signaling. J Exp Biol. 2003; 206:1985–1992. [PubMed: 12756280]

Chang DT, Honick AS, Reynolds IJ. Mitochondrial trafficking to synapses in cultured primary cortical neurons. J Neurosci. 2006; 26:7035–7045. [PubMed: 16807333]

Choeiri C, Staines W, Messier C. Immunohistochemical localization and quantification of glucose transporters in the mouse brain. Neuroscience. 2002; 111:19–34. [PubMed: 11955709]

Cole RN, Hart GW. Cytosolic O-glycosylation is abundant in nerve terminals. J Neurochem. 2001; 79:1080–1089. [PubMed: 11739622]

Dash MB, Bellesi M, Tononi G, Cirelli C. Sleep/wake dependent changes in cortical glucose concentrations. J Neurochem. 2013; 124:79–89. [PubMed: 23106535]

Ferreira JM, Burnett AL, Rameau GA. Activity-dependent regulation of surface glucose transporter-3. J Neurosci. 2011; 31:1991–1999. [PubMed: 21307237]

Fort AG, Murray JW, Dandachi N, Davidson MW, Dermietzel R, Wolkoff AW, Spray DC. In vitro motility of liver connexin vesicles along microtubules utilizes kinesin motors. J Biol Chem. 2011; 286:22875–22885. [PubMed: 21536677]

Gerhart DZ, Broderius MA, Borson ND, Drewes LR. Neurons and microvessels express the brain glucose transporter protein GLUT3. Proc Natl Acad Sci U S A. 1992; 89:733–737. [PubMed: 1731347]

Glater EE, Megeath LJ, Stowers RS, Schwarz TL. Axonal transport of mitochondria requires milton to recruit kinesin heavy chain and is light chain independent. J Cell Biol. 2006; 173:545–557. [PubMed: 16717129]

Hall CN, Klein-Flugge MC, Howarth C, Attwell D. Oxidative phosphorylation, not glycolysis, powers presynaptic and postsynaptic mechanisms underlying brain information processing. J Neurosci. 2012; 32:8940–8951. [PubMed: 22745494]

Hart GW, Slawson C, Ramirez-Correa G, Lagerlof O. Cross talk between O-GlcNAcylation and phosphorylation: roles in signaling, transcription, and chronic disease. Annu Rev Biochem. 2011; 80:825–858. [PubMed: 21391816]

Hornbeck PV, Kornhauser JM, Tkachev S, Zhang B, Skrzypek E, Murray B, Latham V, Sullivan M. PhosphoSitePlus: a comprehensive resource for investigating the structure and function of experimentally determined post-translational modifications in man and mouse. Nucleic Acids Res. 2012; 40:D261–270. [PubMed: 22135298]

Hou BH, Takanaga H, Grossmann G, Chen LQ, Qu XQ, Jones AM, Lalonde S, Schweissgut O, Wiechert W, Frommer WB. Optical sensors for monitoring dynamic changes of intracellular metabolite levels in mammalian cells. Nat Protoc. 2011; 6:1818–1833. [PubMed: 22036884]

Huang CW, Huang CC, Cheng JT, Tsai JJ, Wu SN. Glucose and hippocampal neuronal excitability: role of ATP-sensitive potassium channels. J Neurosci Res. 2007; 85:1468–1477. [PubMed: 17410601]

Iyer SP, Akimoto Y, Hart GW. Identification and cloning of a novel family of coiled-coil domain proteins that interact with O-GlcNAc transferase. J Biol Chem. 2003; 278:5399–5409. [PubMed: 12435728]

Iyer SP, Hart GW. Roles of the tetratricopeptide repeat domain in O-GlcNAc transferase targeting and protein substrate specificity. J Biol Chem. 2003; 278:24608–24616. [PubMed: 12724313]

Ji S, Kang JG, Park SY, Lee J, Oh YJ, Cho JW. O-GlcNAcylation of tubulin inhibits its polymerization. Amino Acids. 2010; 40:809–818. [PubMed: 20665223]

Kang JS, Tian JH, Pan PY, Zald P, Li C, Deng C, Sheng ZH. Docking of axonal mitochondria by syntaphilin controls their mobility and affects short-term facilitation. Cell. 2008; 132:137–148. [PubMed: 18191227]

Khidekel N, Ficarro SB, Clark PM, Bryan MC, Swaney DL, Rexach JE, Sun YE, Coon JJ, Peters EC, Hsieh-Wilson LC. Probing the dynamics of O-GlcNAc glycosylation in the brain using quantitative proteomics. Nat Chem Biol. 2007; 3:339–348. [PubMed: 17496889]

Lazarus MB, Nam Y, Jiang J, Sliz P, Walker S. Structure of human O-GlcNAc transferase and its complex with a peptide substrate. Nature. 2011; 469:564–567. [PubMed: 21240259]

Li Y, Lim S, Hoffman D, Aspenstrom P, Federoff HJ, Rempe DA. HUMMR, a hypoxia- and HIF-1alpha-inducible protein, alters mitochondrial distribution and transport. J Cell Biol. 2009; 185:1065–1081. [PubMed: 19528298]

Liesa M, Shirihai OS. Mitochondrial dynamics in the regulation of nutrient utilization and energy expenditure. Cell Metab. 2013; 17:491–506. [PubMed: 23562075]

Liu X, Hajnoczky G. Altered fusion dynamics underlie unique morphological changes in mitochondria during hypoxia-reoxygenation stress. Cell Death Differ. 2011; 18:1561–1572. [PubMed: 21372848]

Lopez-Domenech G, Serrat R, Mirra S, D'Aniello S, Somorjai I, Abad A, Vitureira N, Garcia-Arumi E, Alonso MT, Rodriguez-Prados M, et al. The Eutherian Armcx genes regulate mitochondrial trafficking in neurons and interact with Miro and Trak2. Nat Commun. 2012; 3:814. [PubMed: 22569362]

Love DC, Hanover JA. The hexosamine signaling pathway: deciphering the "O-GlcNAc code". Sci STKE. 2005; 2005:re13. [PubMed: 16317114]

Macaskill AF, Rinholm JE, Twelvetrees AE, Arancibia-Carcamo IL, Muir J, Fransson A, Aspenstrom P, Attwell D, Kittler JT. Miro1 is a calcium sensor for glutamate receptor-dependent localization of mitochondria at synapses. Neuron. 2009; 61:541–555. [PubMed: 19249275]

Matthews JA, Belof JL, Acevedo-Duncan M, Potter RL. Glucosamine-induced increase in Akt phosphorylation corresponds to increased endoplasmic reticulum stress in astroglial cells. Mol Cell Biochem. 2007; 298:109–123. [PubMed: 17136481]

Nie D, Sahin M. A genetic model to dissect the role of Tsc-mTORC1 in neuronal cultures. Methods Mol Biol. 2011; 821:393–405. [PubMed: 22125080]

Nunnari J, Suomalainen A. Mitochondria: in sickness and in health. Cell. 2012; 148:1145–1159. [PubMed: 22424226]

Park JH, Schroeder AJ, Helfrich-Forster C, Jackson FR, Ewer J. Targeted ablation of CCAP neuropeptide-containing neurons of Drosophila causes specific defects in execution and circadian timing of ecdysis behavior. Development. 2003; 130:2645–2656. [PubMed: 12736209]

Pathak D, Sepp KJ, Hollenbeck PJ. Evidence that myosin activity opposes microtubule-based axonal transport of mitochondria. J Neurosci. 2010; 30:8984–8992. [PubMed: 20592219]

Peppiatt C, Attwell D. Neurobiology: feeding the brain. Nature. 2004; 431:137–138. [PubMed: 15356612]

Pilling AD, Horiuchi D, Lively CM, Saxton WM. Kinesin-1 and Dynein are the primary motors for fast transport of mitochondria in Drosophila motor axons. Mol Biol Cell. 2006; 17:2057–2068. [PubMed: 16467387]

Ruan HB, Han X, Li MD, Singh JP, Qian K, Azarhoush S, Zhao L, Bennett AM, Samuel VT, Wu J, et al. O-GlcNAc transferase/host cell factor C1 complex regulates gluconeogenesis by modulating PGC-1alpha stability. Cell Metab. 2012; 16:226–237. [PubMed: 22883232]

Ruan HB, Singh JP, Li MD, Wu J, Yang X. Cracking the O-GlcNAc code in metabolism. Trends Endocrinol Metab. 2013

Saxton WM, Hollenbeck PJ. The axonal transport of mitochondria. J Cell Sci. 2012; 125:2095–2104. [PubMed: 22619228]

Schneider CA, Rasband WS, Eliceiri KW. NIH Image to ImageJ: 25 years of image analysis. Nat Methods. 2012; 9:671–675. [PubMed: 22930834]

Schuldiner O, Berdnik D, Levy JM, Wu JS, Luginbuhl D, Gontang AC, Luo L. piggyBac-based mosaic screen identifies a postmitotic function for cohesin in regulating developmental axon pruning. Dev Cell. 2008; 14:227–238. [PubMed: 18267091]

Schwarz TL. Mitochondrial trafficking in neurons. Cold Spring Harb Perspect Biol. 2013:5.

Silver IA, Erecinska M. Extracellular glucose concentration in mammalian brain: continuous monitoring of changes during increased neuronal activity and upon limitation in oxygen supply in normo-, hypo-, and hyperglycemic animals. J Neurosci. 1994; 14:5068–5076. [PubMed: 8046468]

Stowers RS, Megeath LJ, Gorska-Andrzejak J, Meinertzhagen IA, Schwarz TL. Axonal transport of mitochondria to synapses depends on milton, a novel Drosophila protein. Neuron. 2002; 36:1063–1077. [PubMed: 12495622]

Tallent MK, Varghis N, Skorobogatko Y, Hernandez-Cuebas L, Whelan K, Vocadlo DJ, Vosseller K. In vivo modulation of O-GlcNAc levels regulates hippocampal synaptic plasticity through interplay with phosphorylation. J Biol Chem. 2009; 284:174–181. [PubMed: 19004831]

Trinidad JC, Barkan DT, Gulledge BF, Thalhammer A, Sali A, Schoepfer R, Burlingame AL. Global identification and characterization of both O-GlcNAcylation and phosphorylation at the murine synapse. Mol Cell Proteomics. 2012; 11:215–229. [PubMed: 22645316]

van Spronsen M, Mikhaylova M, Lipka J, Schlager MA, van den Heuvel DJ, Kuijpers M, Wulf PS, Keijzer N, Demmers J, Kapitein LC, et al. TRAK/Milton Motor-Adaptor Proteins Steer Mitochondrial Trafficking to Axons and Dendrites. Neuron. 2013; 77:485–502. [PubMed: 23395375]

Visscher K, Schnitzer MJ, Block SM. Single kinesin molecules studied with a molecular force clamp. Nature. 1999; 400:184–189. [PubMed: 10408448]

Wang X, Schwarz TL. Imaging axonal transport of mitochondria. Methods Enzymol. 2009a; 457:319–333. [PubMed: 19426876]

Wang X, Schwarz TL. The mechanism of Ca2+-dependent regulation of kinesin-mediated mitochondrial motility. Cell. 2009b; 136:163–174. [PubMed: 19135897]

Wang X, Winter D, Ashrafi G, Schlehe J, Wong YL, Selkoe D, Rice S, Steen J, LaVoie MJ, Schwarz TL. PINK1 and Parkin target Miro for phosphorylation and degradation to arrest mitochondrial motility. Cell. 2011; 147:893–906. [PubMed: 22078885]

Weisova P, Concannon CG, Devocelle M, Prehn JH, Ward MW. Regulation of glucose transporter 3 surface expression by the AMP-activated protein kinase mediates tolerance to glutamate excitation in neurons. J Neurosci. 2009; 29:2997–3008. [PubMed: 19261894]

Yi W, Clark PM, Mason DE, Keenan MC, Hill C, Goddard WA 3rd, Peters EC, Driggers EM, Hsieh-Wilson LC. Phosphofructokinase 1 glycosylation regulates cell growth and metabolism. Science. 2012; 337:975–980. [PubMed: 22923583]

Zala D, Hinckelmann MV, Yu H, Lyra da Cunha MM, Liot G, Cordelieres FP, Marco S, Saudou F. Vesicular glycolysis provides on-board energy for fast axonal transport. Cell. 2013; 152:479–491. [PubMed: 23374344]

HIGHLIGHTS

- Increasing extracellular glucose selectively decreases mitochondrial movement
- Milton *O*-GlcNAcylation by OGT modulates mitochondrial motility
- Milton *O*-GlcNAcylation mediates the effect of extracellular glucose.
- OGT, by responding to altered nutrient states, can regulate mitochondrial dynamics

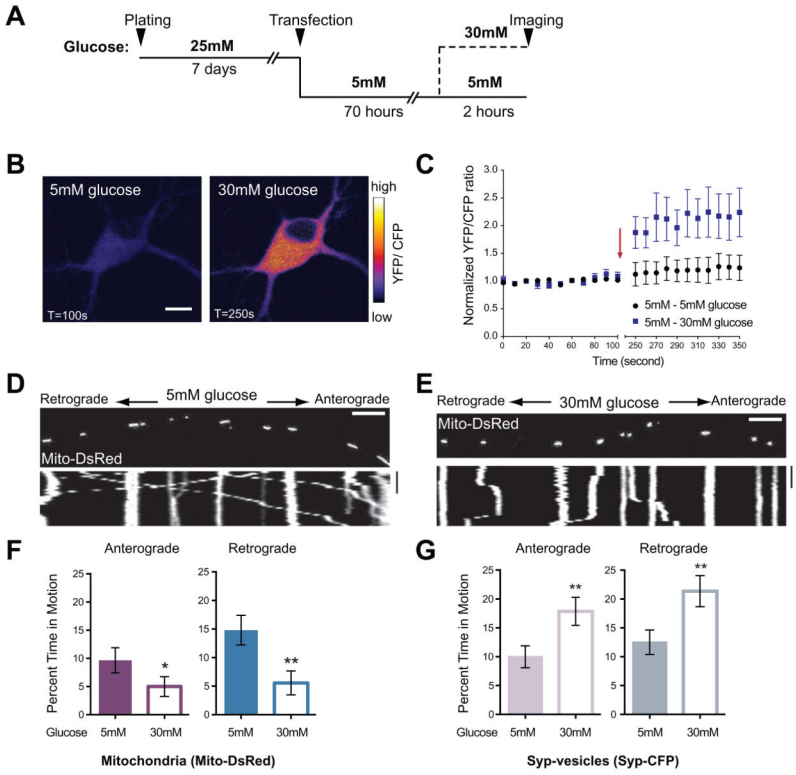

Figure 1. Increased Glucose Decreases Mitochondrial Motility In Rat Hippocampal Axons

(A) Schematic of the paradigm for changing extracellular glucose.

(B–C) The sensor FLII^{12}Pglu-600μδ6 was expressed in cultured rat hippocampal neurons and the YFP/CFP ratio used to determine intracellular glucose concentration in 5mM and after switching 30mM glucose medium. (B) Pseudocolored pixel by pixel ratio of a neuron before and after the switch to 30mM glucose (scale bar =10μm). (C) Normalized YFP/CFP ratios from neurons cultured in 5mM glucose before and after exchange (arrow) of medium for either fresh 5mM glucose (●) or 30mM glucose. (■). 30mM extracellular glucose caused ~2 fold increase in intracellular glucose (p=0.0007, n>4, 3 independent transfections).

(D–E) Representative kymographs of mitochondrial motility in hippocampal axons transfected with Mito-DsRed and Synaptophysin (Syp)-CFP and imaged after culturing as schematized in (A). Here and in subsequent figures, the first frame of each time-lapse movie is shown above a kymograph generated from that region of axon. The y-axis of each kymograph represents time and the x-axis depicts the position of the organelles such that stationary organelles appear as vertical lines while those moving either anterograde or retrograde are diagonal. Scale bars = 10μm and 100s.

(F–G) The percent time each mitochondrion (F) or Syp-vesicle (G) spent in anterograde and retrograde motion was calculated from kymographs like those in (D–E). n=73–101 mitochondria from 8 axons and n=114–126 vesicles from 7 axons and 4 independent transfections per condition.

*p< 0.05, **p<0.01, Mann-Whitney *U* test. All values are shown as mean ± SEM. See also Movies S1–S4 and Table S1.

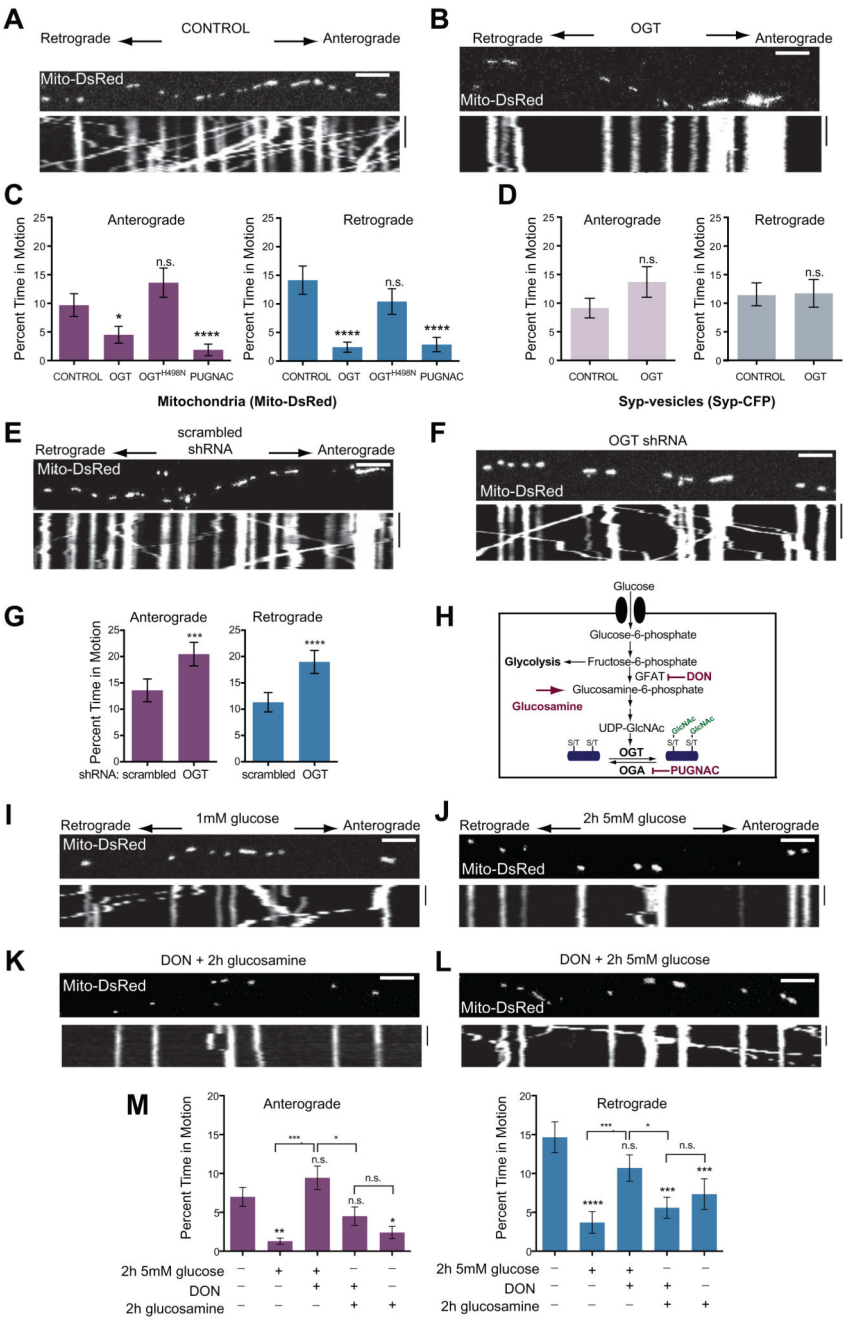

Figure 2. OGT and the Hexosamine Pathway Inhibit Mitochondrial Motility

(A–D) Kymographs of axons from hippocampal neurons transfected with Mito-DsRed and Syp-CFP, and either with (A) or without (B) OGT, and imaged 3 days after the transfection. (C, D) The percent of time mitochondria (C) and Syp-vesicles (D) spent in motion was quantified from kymographs of either control cultures, or neurons transfected with either OGT or the catalytically inactive OGT^{H498N} or neurons pretreated for 6hrs with 100μM PUGNAC. n=100–129 mitochondria from 8 axons and n=118–165 vesicles from 7–8 axons and 4 independent transfections per condition.

(E–G) Hippocampal neurons were transfected with Mito-DsRed and either a scrambled shRNA (E) or OGT shRNA (F), imaged 4 days after the transfection, and their consequences for mitochondrial motility were quantified (G). n=175–179 mitochondria from 9 axons and 3 independent transfections per condition.

(H) Schematic representation of glucose and glucosamine metabolism by the Hexosamine Biosynthetic Pathway. Rate limiting steps and the inhibitors used in this study are also indicated.

(I–M) Hippocampal neurons, cultured in 5mM glucose were transfected with Mito-DsRed and transferred to media containing 1mM glucose for 48h (similar to Figure 1A). Mitochondrial motility was imaged with the indicated glucose, glucosamine and DON treatments. (I, J) Representative kymograph at 1mM glucose and 2h after shift to 5mM glucose. (K, L) Addition of the GFAT inhibitor DON (100μM) prevented the reduction in motility caused by 5mM glucose (L) but not by 2h exposure to 1mM glucose and 4mM glucosamine (K). (M) Mitochondrial motility was quantified from kymographs as in (I – L). Throughout the experiments in (I–M) medium was supplemented with 1mM lactate and 1mM pyruvate, n=116–199 mitochondria from 8–13 axons and 3–4 independent transfections per condition.

n.s. not significant. *p< 0.05, **p<0.01, ***p<0.001, ****p<0.0001; Kruskal-Wallis test. All values are shown as mean ± SEM. Scale bars = 10μm and 100s. See also Figure S2, Movies S5–S6 and Table S1B.

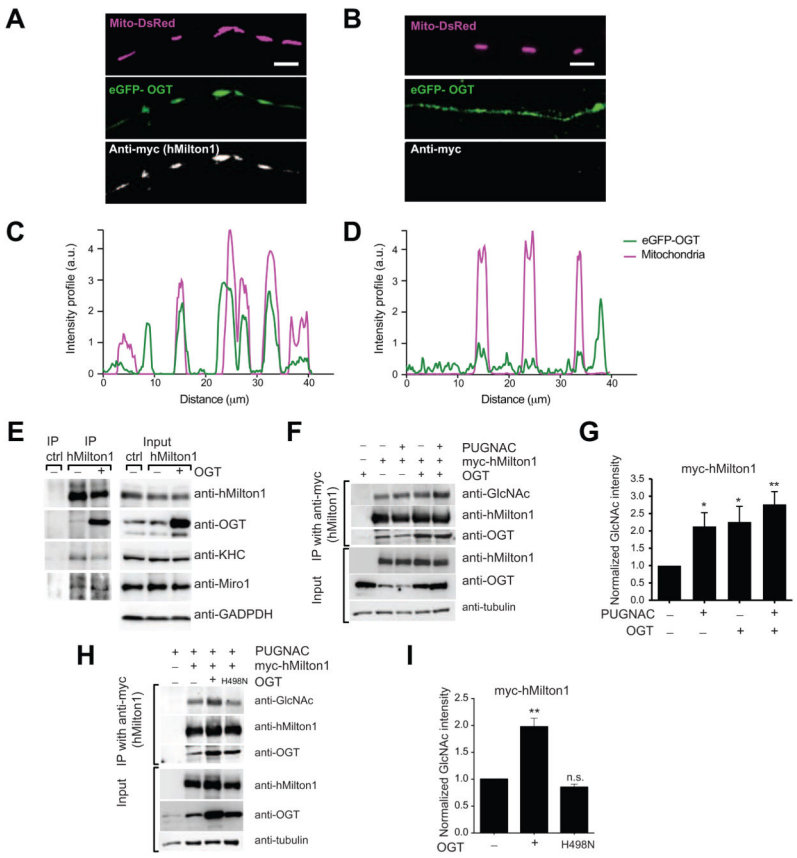

Figure 3. OGT and OGA regulate hMilton1 *O*-GlcNAcylation

(A–D) Milton expression recruits OGT to axonal mitochondria. Hippocampal axons were co-transfected with eGFP–OGT, Mito-DsRed, and either an empty vector (A, C) or myc-hMilton1 (B, D) and immunofluorescent intensity for eGFP-OGT and Mito-DsRed was measured along the length of the axons shown.

(E) Immunoprecipitation (IP) of endogenous hMilton1 from HEK293T cells to analyze the consequences of OGT overexpression. Precipitation with rabbit IgG was used as a control. Input lanes were loaded with 3% of the cell lysates used for the IP and also probed with anti-GAPDH antibody as a loading control. OGT overexpression increased its coprecipitation with Milton without decreasing the presence of Miro or KHC in the complex. A lower OGT-immunoreactive band in the input lanes arises from the intramitochondrial isoform of OGT, which is not co-precipated with hMilton1.

(F–I) Regulation of hMilton1 *O*-GlcNAcylation in HEK293T cells. Cells were transfected and treated as indicated. (F) myc-hMilton1 was immunoprecipitated with anti-myc from cells treated overnight with 100μM PUGNAC and/or overexpressing OGT. With fluorescently tagged secondary antibodies, band intensities were quantified (G) in the linear range and the intensity of each GlcNAc band was normalized to the intensity of myc bands. GlcNAc levels on myc-hMilton1 in untreated cells was set as 1 and fold changes in response to PUGNAC treatment and OGT overexpression were calculated. n=4 independent transfections per condition. (H, I) myc-hMilton1 was immunoprecipitated from HEK293T

cells with or without overexpression of OGT or catalytically dead OGT^{H498N} and its GlcNAcylation quantified as in (G). n=3 independent transfections per condition. n.s. not significant. *p< 0.05, **p<0.01, One-way ANOVA. All values are shown as mean ± SEM. Scale bar represents 10μm. See also Figure S3.

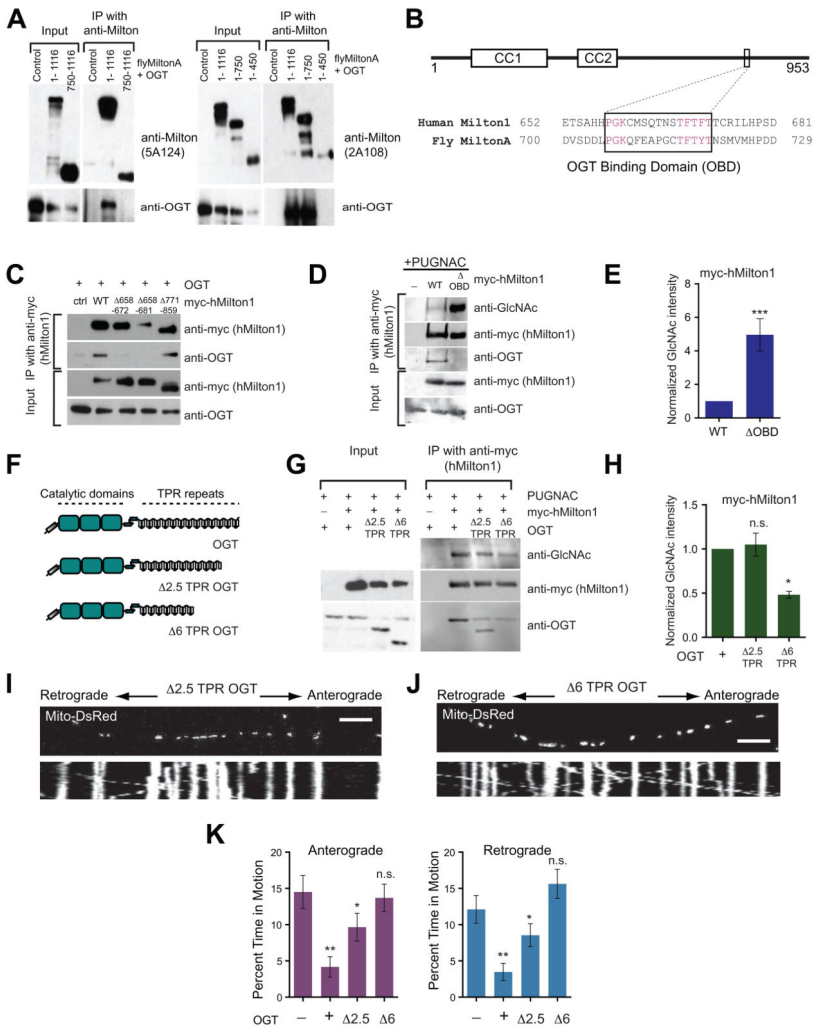

Figure 4. An OGT/Milton Complex Is Not Required for hMilton1 *O*-GlcNAcylation

(A) Coimmunoprecipitation of full length or truncated fly MiltonA and OGT proteins from HEK293T cells. Anti-Drosophila Milton antibodies 5A124 (raised against amino acids 908–1055) or 2A108 (raised against amino acids 273–450) were used to immunoprecipitate full length (1–1116) or truncated 750–1116, 1–750, and 1–450 Drosophila MiltonA. Immunoblots were probed with anti-OGT and the appropriate anti-Milton antibodies to identify Milton fragments that could associate with OGT.

(B) Schematic representation of hMilton1 protein and sequence alignment of fly MiltonA (450–750) and hMilton1 (634–953) (see also Figure S4), which were determined to be important for OGT/Milton complex formation. The conserved OGT Binding Domain (OBD) is boxed; conserved amino acids are magenta. Predicted coiled coil domains of hMilton1 (CC1,2) are also illustrated.

(C) Myc-hMilton1 constructs lacking the indicated amino acids were tested for their ability to precipitate coexpressed OGT from HEK293T cells.

(D–E) Full length and Δ658–672 (ΔOBD) hMilton1 were immunoprecipitated from 100μM PUGNAC-treated HEK293T cells and *O*-GlcNAcylation was quantified as in Figure 3. Loss

of the high-affinity interaction increased Milton *O*-GlcNAcylation. n≥3 independent transfections per condition.

(F-H) Full length and truncated OGT constructs lacking either the first 2.5 or 6 TRP motifs (Δ2.5, Δ6 as shown in F) were coexpressed in HEK293T cells with full length hMilton1 (WT) to evaluate the significance of the TPR motifs on OGT/Milton complex formation and the level of hMilton1 *O*-GlcNAcylation. myc-hMilton1 was immunoprecipitated and immunoblots were analyzed with anti-GlcNAc, anti-myc and anti-OGT. n=3 independent transfections per condition.

(I–K) Hippocampal neurons were transfected with Mito-DsRed and either full length or Δ2.5 or Δ6 truncated OGT and imaged 3 days after transfection. From kymographs as in (I and J), mitochondrial motility was quantified (K) and compared with control. n=111–209 mitochondria from 10–12 axons and 3 independent transfections per condition. n.s. not significant. *p< 0.05, **p<0.01; One-way ANOVA, Kruskal-Wallis test. All values are shown as mean ± SEM. Scale bar represents 10μm and 100s. See also Figure S3 and Table S1C.

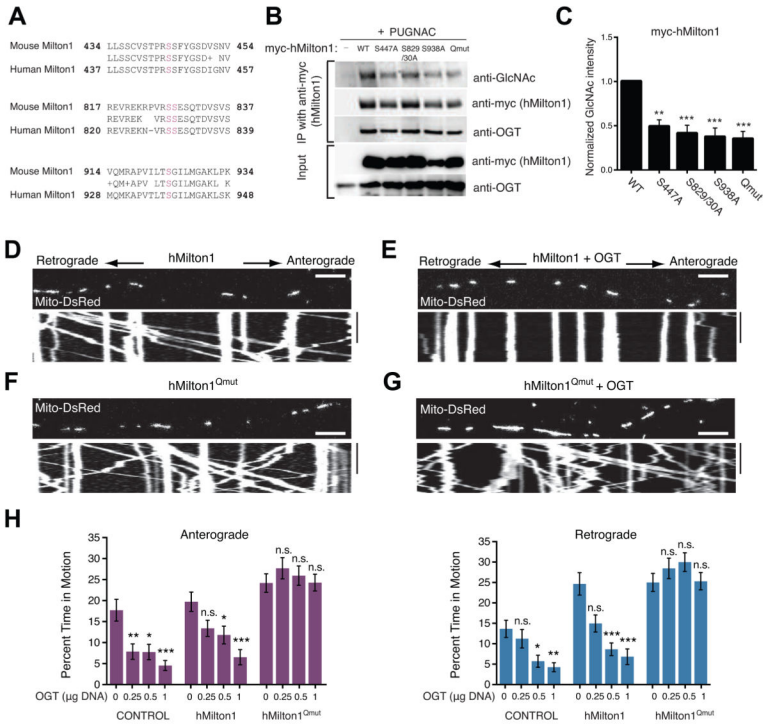

Figure 5. OGT-Dependent Mitochondrial Motility Arrest Requires Milton *O*-GlcNAcylation

(A) Sequence alignment of *O*-GlcNAcylation sites (magenta) in mouse Milton1 with homologous regions in hMilton1 (see also Figure S5 and Table S1D).

(B–C) Myc-hMilton1 with either individual putative GlcNAc sites mutated, or the quadruple mutant lacking all four sites (Qmut) or wildtype (WT) were expressed in HEK293T cells and cultured overnight with 100µM PUGNAC. Milton immunoprecipitates were probed with anti-GlcNAc, anti-myc and anti-OGT antibodies and GlcNAcylation levels on Milton were quantified with fluorescently tagged secondary antibodies. The intensity of each GlcNAc band was normalized to the intensity of the myc band, with the baseline hMilton1 GlcNAc level set as 1 to reveal relative changes. n≥3 independent transfections per condition.

(D–G) Hippocampal neurons were transfected with Mito-DsRed and the indicated forms of hMilton1, with (E and G) or without (D and F) OGT (0.5 µg OGT DNA/well). Mitochondrial motility was imaged 3 days after transfection. (H) To assess the effect of the mutated GlcNAcylation sites, a dose/response relationship was established with different levels of DNA for OGT transfection and its effect on mitochondrial motility quantified from kymographs as in (D–G). The amount of OGT DNA transfected per well of a 24-well plate is indicated. n=75–174 mitochondria from 8–9 axons and 3 independent transfections per condition. All values are shown as mean ± SEM. The significance of changes in motility was determined relative to the motility in neurons expressing the same Milton construct without OGT transfection. n.s. not significant. *p< 0.05, **p<0.01, ***p<0.001; One-way ANOVA, Kruskal-Wallis test. Scale bar represents 10µm and 100s. See also Figure S5, Movies S7–S8 and Table S1E.

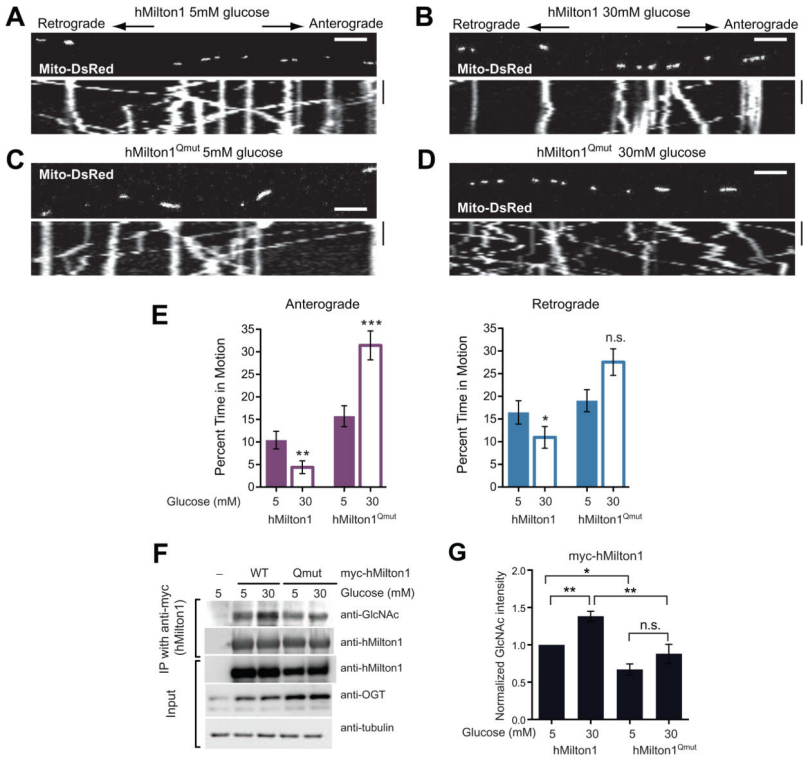

Figure 6. Milton *O*-GlcNAcylation Is Necessary for Glucose to Decrease Mitochondrial Movement

(A–D) Hippocampal neurons were transfected with Mito-DsRed, and either WT or Qmut hMilton1 constructs as indicated and cultured as per the protocol described in Figure 1A.

(E) Percent time each mitochondrion spent in anterograde and retrograde motion was calculated from kymographs as in (A – D). n=105–135 mitochondria from 9 axons and 3 independent transfections per condition. Scale bar represents 10μm and 100s. See also Table S1F.

(F–G) WT or Qmut myc-hMilton1 were expressed in HEK293T cells cultured in 25mM glucose containing DMEM. Glucose levels were then lowered to 5mM for 24hrs before challenging them with 30mM or 5mM glucose for 2hrs, as in the motility experiments. Milton immunoprecipitates were probed with anti-GlcNAc, anti-myc and anti-OGT antibodies (F) and GlcNAcylation levels on Milton were quantified (G). n=4 independent transfections per condition.

All values are shown as mean ± SEM. n.s. not significant. *p< 0.05, **p<0.01, ***p<0.001; Mann-Whitney *U* test, One-way ANOVA.

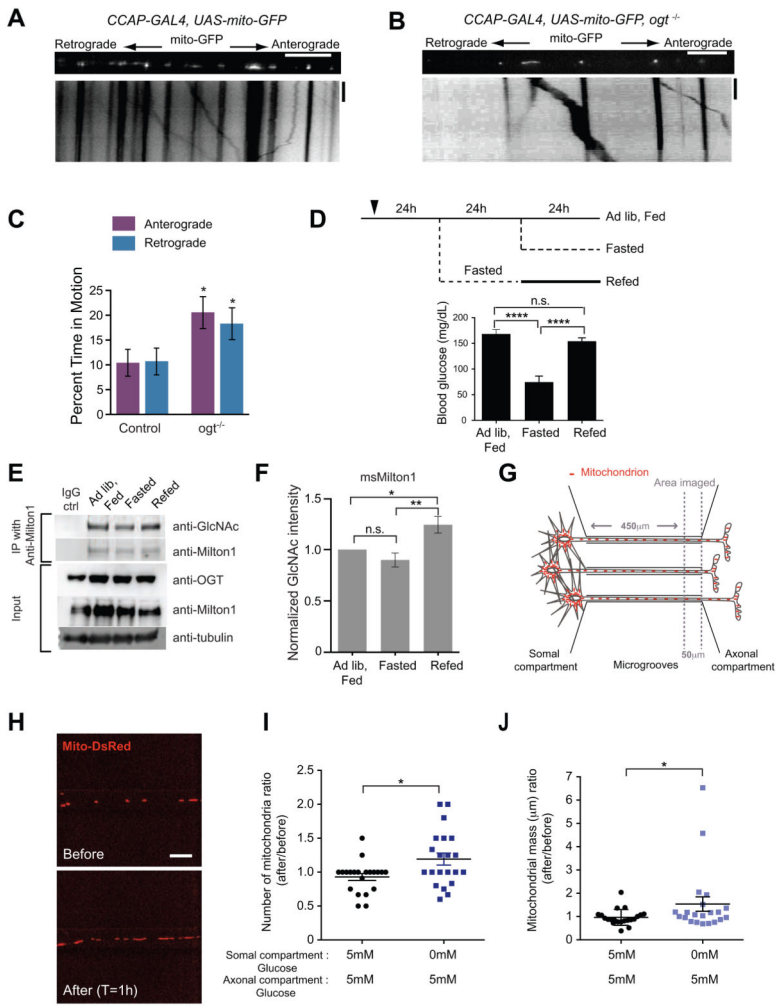

Figure 7. Evidence of OGT-Dependent Regulation of Milton *O*-GlcNAcylation *in vivo*

(A–B) In control and ogt$^{-/-}$ larvae UAS-mito-GFP was expressed in an identified peptidergic axon within the segmental nerve by CCAP-GAL4. (C) The percent time each mitochondrion spent in anterograde and retrograde motion was calculated from kymographs as in (A and B). n=91–100 mitochondria from 9 axons from 9 animals. Scale bar represents 10μm and 100s.

(D) Schematic of the experimental regimen for changing blood glucose levels by fasting and re-feeding and measured blood glucose levels from the mice that were used to compare Milton *O*-GlcNAcylation levels in the brain.

(E–F) Immediately after blood glucose measurements, two cortical hemispheres were removed and homogenized. Milton1 was immunoprecipitated (E) and GlcNAcylation levels on Milton were quantified (F). n=6 pairs of animals.

(G) Schematic of the microfluidic-based culture platform. The culture chamber consists of fluidically isolated somal and axonal compartments connected by microgrooves. Glucose levels in the axonal and somal compartments were independently manipulated and mitochodria were imaged in a 50μm length of axon at the proximal end of the axonal compartment.

(H–J) Hippocampal neurons, cultured in microfludic devices in 5mM glucose (with 1mM lactate and pyruvate), were transfected with Mito-DsRed. The medium in the somal compartment was replaced with either the same solution or with a glucose-free medium (with 1mM lactate and pyruvate). The same axons were imaged both before and 1h after this solution change (H) so that its effect on mitochondrial density and mass could be quantified (I–J). n= 21 axons, 4 microfluidic devices per condition, 3 independent experiments.
All values are shown as mean ± SEM. n.s. not significant. *p< 0.05, ****p<0.0001, Mann-Whitney *U* test, One-way ANOVA, Kruskal-Wallis test. See also Figure S6.